Use of a laser energy source in producing a reactive thrust

F. V. Bunkin and A. M. Prokhorov

P. N. Lebedev Physics Institute, USSR Academy of Sciences, Moscow
Usp. Fiz. Nauk **119**, 425–446 (July 1976)

The physical principles are given of laser jet engines, in which the source of energy ("fuel") is a laser source of electromagnetic energy located outside the flight vehicle being accelerated. An analysis is made of two mechanisms of producing a thrust: one is the evaporation mechanism involving the evaporation of the propulsive mass of the flight vehicle by the incident laser radiation and the other is the "explosive" mechanism due to the laser-induced breakdown of air ("explosion") and excitation of a shock wave which can propel the flight vehicle. The first mechanism can be used in the atmosphere and in space, whereas the second can be used only in the atmosphere (laser air-breathing jet engine). The main characteristics of laser jet engines (the ratio of the laser power to the thrust obtained, specific impulse, and power conversion efficiency) are obtained and some of them are confirmed experimentally. The promising nature of the use of lasers in jet engines of this kind is stressed.

PACS numbers: 42.60.Qm, 89.40.+k, 93.20.+r

CONTENTS

1. INTRODUCTION

Askar'yan and Moroz[1] were the first to draw attention to the reactive impulse due to the ejection of a vapor from a target acted upon by sufficiently strong laser radiation. The evaporation mechanism of the reactive recoil in pulse irradiation of solid targets of various physicochemical compositions was investigated theoretically and experimentally in several papers (see, for example, [2–5]). Kantrowitz[6] suggested the use of the thrust resulting from the evaporation of a solid propellant of a rocket for acceleration of flight vehicles (in particular, for launching them into an earth satellite orbit) by a ground-based laser energy source. The main ideas of such a laser jet engine were developed more fully by Pirri, Monsler, and Nebolsine.[7]

However, the evaporation thrust mechanism is not the only possible approach in the utilization of a laser energy source for reactive acceleration of flight vehicles. The laser jet engine discussed in[6,7] is analogous to a conventional solid-fuel rocket engine except that in the former the surface heating and evaporation of the propulsive mass ("fuel") occurs as a result of surface absorption of electromagnetic radiation and not because of self-sustaining combustion (oxidation) as in solid-fuel rockets. However, the energy of the radiation transmitted to a flight vehicle by a laser beam can also be used to heat the propulsive mass of a rocket by other mechanisms. For example, one can readily conceive a laser jet engine similar to a conventional liquid-fuel rocket except that the oxidant is now replaced by laser radiation heating an atomized liquid propellant.

We can see that the principal difference between the laser and conventional jet engines is that in the former case the propulsive mass need not be a chemical fuel. We can say that in a laser jet engine the "fuel" is supplied continuously from outside in the form of radiation energy (during the operation of the engine) but is not carried on board the flight vehicle, as is the case in conventional jet engines. The position of an energy source heating the propulsive mass of a rocket outside the flight vehicle distinguishes in a basic manner a laser jet engine from electrojet engines investigated recently in which the source of electrical energy is on board the vehicle.

The supply of a "fuel" in the form of radiation energy from outside makes a laser jet engine particularly attractive for its use in the atmosphere. We are speaking here of laser air-breathing jet engines designed for the acceleration of flight vehicles in the terrestrial atmosphere in which the only propellant would be atmospheric air heated efficiently by laser radiation sent from the ground or from another flight vehicle.[8]

The present paper develops the physical ideas and considers the phenomena underlying the operation of two specific variants of a laser jet engine, one of which has a solid propulsive mass and utilizes the evaporation thrust mechanism (Sec. 2) and the other is an air-breathing jet engine with a pulse-periodic laser and the "explosive" thrust mechansim (Sec. 3). The degrees of development of even the physical ideas underlying these two variants of the laser jet engine are quite different. The evaporation mechanism of reactive recoil, which applies to irradiation of solid targets, has been investigated for over a decade apart from the problem of laser jet engines (see the papers cited above). The

main physical phenomena have been thoroughly investigated and our problem is to present, from a different point of view, the results already known in principle and on this basis to establish the fundamental characteristics of a laser jet engine with the evaporation thrust mechanism. In the case of a laser air-breathing jet engine the very idea of such an engine is new [7,8] and it is based on new physical results obtained in studies of the interaction of CO_2 laser radiation pulses with solid targets in a gaseous atmosphere. [7,9-16] Therefore our presentation of the physical basis of laser air-breathing jet engines will be largely original.

We shall conclude (Sec. 4) by summarizing the discussion and considering the prospects of practical laser jet engines.

2. SOLID-PROPELLANT LASER JET ENGINE WITH EVAPORATION THRUST MECHANISM

A. Physical basis of advanced evaporation of solids by radiation

When the surface of an opaque solid (a target) receives electromagnetic radiation flux and the density of this flux (intensity) is sufficiently high, a process known as "advanced evaporation" of the target is observed. Qualitatively, this process is characterized by the fact that the evolution of energy in the surface layer of the target due to the absorption of the incident radiation is so rapid that this layer becomes evaporated before heat conduction and other heat-transfer processes are able to remove the heat evolved in the surface layer. Thus, under advanced evaporation conditions all the radiation energy absorbed in a target is used to evaporate it. Then, the mass density of the vapor flux j from the target surface is given by a formula which follows from the law of conservation of energy:

$$j=\frac{(1-R)I}{q}, \tag{2.1}$$

where I is the intensity of the radiation reaching the target surface, R is the reflection coefficient of this surface, and q is the specific (per unit mass) heat of evaporation of the target material [the energy needed to heat the target surface to the evaporation temperature and the vapor energy are ignored in Eq. (2.1), which is always justifiable in the case under discussion].

The vapor flux density j is governed, for given thermal properties of the target material and a given external pressure p_e of the gas in which the target is located, by the temperature of the target surface T. If the dependence $j(T)$ is known, the ratio (2.1) can be regarded as an equation describing a steady-state surface temperature T which is a function of the intensity I of the radiation incident on it and causing advanced evaporation, i.e., it is assumed that $I>I_{ev}$, where I_{ev} is the threshold intensity needed for evaporation. The threshold value of I_{ev} depends not only on the thermal properties of the target and the external pressure p_e, but also it generally depends on the ratio of the geometric dimensions of the target to the laser beam diameter d. In the case of a laser jet engine the main interest lies in the situation when the beam diameter d is close to the transverse size of the target (the beam "covers" the surface of the propulsive mass of the engine facing the laser source; see Fig. 1 below) and the thickness l of the target is such that during the time t_{st} needed to establish advanced evaporation the energy supplied to the target cannot penetrate to the opposite surface, i.e., $(\sqrt{\chi t_{st}}+\mu^{-1})\ll l$ (here, χ is the thermal diffusivity of the target material and μ is the absorption coefficient of the incident radiation). This condition is usually satisfied by bulk (but not by film) targets. Under these conditions the process of heating and evaporation of a target is one-dimensional and the threshold value I_{ev} is independent of the geometric dimensions (it is assumed that the distribution of the intensity across the laser beam is uniform and that the transfer of heat through the side surface of the target can be ignored). We shall consider specifically this case.

If the target is irradiated continuously (i.e., if the irradiation time is $t\gg t_{st}$), the threshold value of I_{ev} clearly corresponds to the minimum (at a given external pressure p_e) temperature of the condensed body–vapor phase transition, i.e., it corresponds to the temperature T_{ev} found from the condition $p_s(T_{ev})=p_e$, where $p_s(T)$ is the saturated vapor pressure of the target material (it is assumed that a target material is a single-component substance and that $p_e<p_{tp}$ is the vapor pressure at the triple-three-phase equilibrium-critical point). If $p_e>p_{tp}$, the advanced evaporation always occurs from the liquid phase and $T_{ev}=T_{bp}(p_e)$, where the latter quantity is the boiling point of the target material at a given external pressure p_e. However, if $p_e<p_{tp}$, the advanced evaporation takes place near the threshold from the solid phase (advanced sublimation) and $T_{ev}=T_{subl}(p_e)$, where the latter quantity is the sublimation temperature at a given external pressure p_e. This is the situation which occurs in the case of graphite at atmospheric (and lower) external pressures because graphite is characterized by $p_{tp}\approx 110$ atm. [1)]

The determination of the dependence $j(T)$ for arbitrary values of the external pressure p_e and temperature T is a fairly difficult gas kinetic problem. However, in our case it is simplified greatly by the fact that, for a small excess over the threshold [$I>I_{ev}$, $T(I)>T_{ev}$], the very strong temperature dependence of the saturated vapor pressure $p_s(T)\propto\exp(-q_1/T)$ (q_1 is the heat of evaporation per particle) leads to the conditions $p_s[T(I)]\gg p_e$. Then, the vapor flux density $j(T)$ differs little from the density of the flux obtained by evaporation in vacuum which is given, at temperatures $T<T_{cr}$, where T_{cr} is the critical temperature of the target material, by the well-known formula (see, for example, [17] § 81):

$$j_{vac}(T)=(1-r)\,p_s(T)\sqrt{\frac{M}{2\pi T}}, \tag{2.2}$$

where $M=A/N_A$ is the mass of the particles (A is the atomic weight and N_A is the Avogadro number) and r is

[1)] It should be noted that if $p_e<p_{tp}$ but the threshold is exceeded considerably ($I/I_{ev}>1$) when $T(I)>T_{tp}$, the advanced evaporation still occurs from the liquid phase.

the coefficient of reflection of these particles from the evaporation surface (for metals $r \ll 1$); here and later, the temperature T is expressed in energy units. As shown in[2] (§ 41), in this case we have $j(T) = \alpha j_{vac}(T)$, where the coefficient α, allowing for the reverse flux of evaporated particles back to the target, depends only on the reflection coefficient r and, in principle, is always less than unity but it is numerically close to it. Its minimum value corresponding to the maximum reverse flux (for $r \ll 1$) is 0.82.[2]

The same strong temperature dependence $p_s(T)$ allows us to use the representation $j(T) = \alpha j_{vac}(T)$ with $\alpha \approx 1$ [which corresponds, strictly speaking, to the condition $p_s(T) \gg p_e$] for estimating also the threshold intensity I_{ev}. It follows from Eqs. (2.1) and (2.2) that

$$I_{ev} = \frac{q}{1-R} j(T_{ev}) = \alpha \frac{1-r}{1-R} q p_e \sqrt{\frac{M}{2\pi T_{ev}}} = \alpha \frac{1-r}{1-R} p_e \frac{q_1}{T_{ev}} \bar{v}_1; \tag{2.3}$$

here, $q_1 = qM$ and $\bar{v}_1 = \sqrt{T_{ev}/2\pi M} = \bar{v}/4$ ($\bar{v}$ is the arithmetic mean velocity of the vapor particles at $T = T_{ev}$). As pointed out above, the temperature T_{ev} in the range $p_e > p_{tp}$ is $T_{bp}(p_e)$, whereas in the range $p_e < p_{tp}$ it is equal to $T_{subl}(p_e)$.

We shall estimate the values of T_{ev} for metals and graphite[2)] at $p_e = 1$ atm. In the case of metals $p_{tp} < 1$ atm and, therefore, we have $T_{ev} = T_{bp}^{(0)}$, where the latter quantity is the normal boiling point; for the majority of metals (such as aluminum, copper, iron, molybdenum, and tungsten), the velocity $\bar{v}_1$ lies within the range $(2-3)\times 10^4$ cm/sec and the ratio $\eta = q_1/T_{bp}^{(0)}$ is within the range 12–16 (for tungsten this ratio is 17.5).[3)] In the case of graphite $T_{ev} = T_{subl}^{(0)} = 3770\ ^\circ\mathrm{K} = 5.2\times 10^{-20}$ J is the normal sublimation temperature; in this case $\bar{v}_1 = 6.4\times 10^4$ cm/sec and the ratio is $\eta = q_1/T_{subl}^{(0)} \approx 46$. Using these data and Eq. (2.3), we obtain $I_{ev} \approx 10^5$ W/cm^2 for metals ($R \approx 0.7$) and $I_{ev} \approx 3\times 10^5$ W/cm^2 for graphite ($R \ll 1$).

It should be noted that, according to Eq. (2.3), the threshold value I_{ev} is independent of the thermal conductivity of the target. This is due to the one-dimensional nature of the target heating and evaporation processes. However, even under one-dimensional conditions the time t_{st} taken to establish steady advanced evaporation generally depends on the thermal conductivity (this is always true of metals and graphite). Therefore, in observations of developed evaporation in the case of pulse irradiation of targets (when, in addition to the condition $I > I_{ev}$, it is also necessary to satisfy another evaporation condition, which is $t_{st}/\tau < 1$), the threshold intensity generally depends on the thermal conductivity of the target. Here, τ is the duration of a laser pulse (in experiments with solid-state lasers the duration is usually $\tau \sim 10^{-3}$ sec or 3×10^{-8} sec). Let us now discuss this aspect in greater detail.

The time t_{st} depends both on the radiation intensity I and on the thermal properties. In the range of values t_{st} where $t_{st} \gg (\mu^2\chi)^{-1}$, we clearly have $(1-R)It_{st} = \rho q\sqrt{\chi t_{st}}$ (ρ is the target material density). If $t_{st} \ll (\mu^2\chi)^{-1}$, the values of t_{st} satisfy a different equation: $(1-R)It_{st} = \rho q/\mu$. Consequently, the dimensionless time constant $\theta_{st} = t_{st}\mu^2\chi$ is given by

$$\theta_{st} = \begin{cases} z^2 & \text{for } z > 3, \\ z & \text{for } z \ll 1, \end{cases} \tag{2.4}$$

where $z = \mu\chi/u_{ev}$, $u_{ev} = (1-R)I/\rho q = j/\rho$ is the steady-state velocity of the target evaporation front. The experiments on metals and graphite correspond to $z > 3$ and those on insulators usually to $z \ll 1$. This follows from the fact that in the case of metals and graphite we have $\mu\chi \sim 3\times 10^4$–$10^6$ cm/sec, whereas for typical insulators ($\mu \lesssim 10^2$ cm^{-1}, $\chi \lesssim 10^{-3}$ cm^2/sec), we have $\mu\chi \lesssim 0.1$ cm/sec, which should be compared with the experimentally determined evaporation front velocities u_{ep} which lie for all these substances in the range 1–10^4 cm/sec in the range of intensities from $I \sim 10^5$ W/cm^2 to $I \sim 10^9$ W/cm^2 (it should be noted that higher values of the intensity usually result in optical breakdown of the vapor, manifested by a spark, and we no longer have pure evaporation; this point is discussed later).

Thus, in the case of metals and graphite (and generally all the substances for which $z > 3$), the additional condition for the observation of advanced evaporation in the pulse regime is $t_{st}/\tau = z^2/\tau\mu^2\chi < 1$ or $I > \rho q\sqrt{\chi/\tau}(1-R)^{-1}$. In addition to the main condition $I > I_{ev}$, this gives the following general condition for the observation of advanced evaporation in the pulse regime: $I > \max[I_{ev}, \rho q\sqrt{\chi/\tau}(1-R)^{-1}]$ which can be expressed approximately thus:

$$I > I_{ev} + \frac{\rho p}{1-R}\sqrt{\frac{\chi}{\tau}} \quad \text{(metals, graphite)}. \tag{2.5a}$$

In the case of insulators ($z \ll 1$) the additional condition becomes $t_{st}/\tau = z/\tau\mu^2\chi < 1$ or $I > \rho q/(1-R)\mu$ and the general condition is correspondingly

$$I > I_{ev} + \frac{\rho q}{1-R}\frac{1}{\mu\tau} \quad \text{(insulators)}. \tag{2.5b}$$

Even in the case of long laser pulses ($\tau \sim 10^{-3}$ sec), the second right-hand term in Eqs. (2.5a) and (2.5b) is usually much greater than the first. In the case of metals and graphite it amounts to about $(2-5)\times 10^6$ W/cm^2 (which is in good agreement with the experimental results: see[2-5]).

We shall now return to the target surface temperature T under advanced evaporation conditions. At the threshold intensity $I = I_{ev}$ the temperature is $T = T_{ev}(p_e) = T_{bp}(p_e)$ or $T_{subl}(p_e)$; If $I > I_{ev}$, the surface temperature rises. As pointed out earlier, the dependence $T = T(I)$ can be determined from Eq. (2.1) by substituting $j = \alpha j_{vac}(T)$. We can now see that as long as the temperature $T(I)$ remains less than the critical target temperature T_{cr}, its rise with increasing I is very slow because of the strong temperature dependence of the pres-

---

[2)] Numerical estimates will be obtained later mainly for these substances because the most expensive experimental data are available for metals and graphite is one of the most promising substances for the use in laser jet engines.

[3)] The constancy of the ratio $\eta = q_1/T_{bp}^{(0)}$ is general (Trouton–Pictet rule) but for metals it is slightly higher than the average value $\eta = 10$–11.

sure $p_s(T)$ [see Eq. (2.2)]. In this temperature range ($T_{ev} < T < T_{cr}$), it follows from Eqs. (2.1), (2.2), and the relationship (see[4])

$$p_s(T) = p_e \exp\left(\frac{q_1}{T_{ev}(p_e)}\right) \exp\left(-\frac{q_1}{T}\right)$$

that

$$\frac{q_1}{T} = \frac{q_1}{T_{ev}} - \ln\frac{I}{I_{ev}} - \ln\sqrt{\frac{T}{T_{ev}}}. \qquad (2.6)$$

The approximate solution of this equation, corresponding to the dropping of the last term on the right-hand side, is

$$T = \frac{T_{ev}}{1-(T_{ev}/q_1)\ln(I/I_{ev})}, \quad T < T_{cr}. \qquad (2.7)$$

It follows from this formula that an increase of the surface temperature by a factor of just 1.6 (which, in the case of $T_{ev} = T_{bp}^{(0)}$ is equivalent to approximate attainment of the critical temperature $T_{cr} \approx 1.6 T_{bp}^{(0)}$, in accordance with the Gulberg–Gouy rule) for metals ($q_1/T_{ev} = 12-15$) corresponds to an excess over the threshold by a factor $I/I_{ev} \approx (1-3)\times 10^2$. According to this formula, when the threshold is exceeded by $I/I_{ev} = 10^2$ the temperature rises by just a factor of 1.1, i.e., if $T_{ev} = T_{subl}^{(0)} = 3770\,^\circ\mathrm{K}$ it gives a temperature of $T \approx 4150\,^\circ\mathrm{K}$ ($\lesssim T_{cr} \approx 4200\,^\circ\mathrm{K}$).

Thus, we reach a very important (particularly in the case of laser jet engines) conclusion that the target surface temperature T under advanced evaporation conditions is independent of the intensity of the incident radiation I in a wide range of this intensity and is essentially governed by the heat of evaporation of the target material q_1. In the case of metals and radiation intensities in the range $10^5 - 3\times 10^7\ \mathrm{W/cm^2}$, the target surface temperature T lies within the range $T_{bp}^{(0)} \lesssim T \lesssim T_{cr} \approx 1.6 T_{bp}^{(0)}$; in the case of graphite an increase in the incident radiation intensity from $I \approx 3\times 10^5\ \mathrm{W/cm^2}$ to $I \approx 3\times 10^7\ \mathrm{W/cm^2}$ increases the temperature from $T \approx 3770\,^\circ\mathrm{K}$ to $T \approx 4150\,^\circ\mathrm{K}$. In the case of laser jet engines the upper limit of this range of intensities ($3\times 10^7\ \mathrm{W/cm^2}$) clearly exceeds considerably the realistic potentialities even when the most optimistic forecasts are made as to the future development of laser technology. Therefore, in considering laser jet engines one should assume intensities of $I \sim 10^5 - 10^6\ \mathrm{W/cm^2}$ and, consequently, temperatures close to $T \approx T_{bp}^{(0)}$ (in the case of graphite we should consider temperatures close to $T_{subl}^{(0)} \approx 3770\,^\circ\mathrm{K}$).

This conclusion seems to be discouraging in application to laser jet engines because there is no longer any serious advantage in using a laser energy source rather than a chemical one: modern rocket fuels make it possible to attain gas mixture temperatures of ~3000–4000 °K in the combustion chamber, i.e., the temperatures are of the same order as those that may be obtained by advanced evaporation on the surfaces of solids with the highest boiling (sublimation) temperatures. However, there is an advantage in the sense of the working temperature of the gas or vapor. This advantage derives from the fact that the working temperature of the vapor in a laser jet engine may be increased considerably (by a factor of 2.5–4.5) using the same laser radiation flux which evaporates the target. We shall now consider this important point in greater detail.

A vapor jet ejected by a target is penetrated by laser radiation falling on the target. There is a certain range of radiation intensities I (the width of this range depends on the wavelength and this point is discussed later) in which the evaporation process is stable, i.e., the vapor interacting with the incident radiation is not converted into a strongly absorbing plasma and there is no significant screening of the target by the vapor. However, this does not mean that the vapor temperature remains equal (or close to) the surface temperature T. In fact, the stable state corresponds to a vapor temperature higher by the factor mentioned above and this is due to the interaction with the radiation. A suitable construction of a laser jet engine may ensure that this higher temperature is the working temperature of the vapor (see Sec. 2b).

Potential heating of a laser jet by radiation can be found on the basis of hydrodynamics of combustion involving an interaction between a moving vapor and electromagnetic (in particular, optical) radiation. As in normal combustion accompanied by a release of the chemical energy, we can have subsonic ("slow combustion") and supersonic ("detonation") regimes of propagation of "optical" discharges. The first ideas on these processes were put forward by Ramsden and Savic[18] ("optical detonation") and by Bunkin *et al.*[19] ("slow combustion of an optical beam"). This part of hydrodynamics has now been developed much further (see Raĭzer's monograph[20]).

We shall assume that the target surface is plane. We shall first ignore the possibility of interaction of the incident radiation with the vapor and consider the nature of motion of the vapor in a region whose linear dimensions are of the same order as the laser beam diameter d (in the case of a laser jet engine, we shall consider a region of the order of the transverse size of the propulsive mass of a rocket; see above and Fig. 1) and we shall assume that this region is adjacent to the target surface. The influence of an external pressure $p_e \lesssim 1$ atm can be ignored (this point is discussed later). From the kinetic point of view, this region is separated from the target being evaporated by a thin Knudsen layer (its thickness amounts to several mean free paths of the vapor particles), beyond which the true hydrodynamic flow of the vapor takes place. In a hydrodynamic analysis the boundary of this layer is a surface of weak discontinuity beyond which a transient vapor rarefaction wave is formed (see, for example, [21] § 92). On the discontinuity surface the velocity of flow is always equal to the local velocity of sound $c_0 = \sqrt{\gamma T_0/M}$ (γ is the constant of the Poisson adiabat of the vapor), the vapor temperature is $T_0 = \beta_1 T$, and its pressure is $p_0 = \beta_2 p_s(T)$, where T is the target surface temperature, β_1 and β_2 are coefficients smaller than unity and dependent on the reverse flux of the evaporated particles back to the target. A kinetic calculation of these coefficients for $r \ll 1$ (for example, metals) gives $\beta_1 \approx 0.65$

and $\beta_2 \approx 0.2$ (see[2], § 4).

The time taken to establish (from the beginning of the evaporation process) the steady-state values of all the hydrodynamic parameters in the vapor flow region under discussion is governed by the condition $t \gg d/c_0$. In the layer of thickness $x \ll d$ adjoining directly the target (x is the distance along the normal to the target surface) the flow of vapor is basically planar and one-dimensional so that the steady-state values of the hydrodynamic parameters are independent of the coordinate x and, in particular, the steady-state velocity of flow in the layer is $u_1 = c_0$. Outside the layer the vapor jet begins to expand laterally and, therefore, the steady-state values of its density ρ_1, pressure p_1, and temperature T_1 decrease monotonically with the coordinate x and the velocity $u_1 = u_1(x)$ rises monotonically from $(u_1)_{\min} = u_1(0) = c_0$; clearly, at all points in this region the flow is supersonic [$u_1(x) > c_1(x) = \sqrt{\gamma T_1(x)/M}$]. However, it should be noted that although in the region $x \lesssim d$ the lateral expansion of vapor jet is slight, the values of ρ_1, p_1, T_1, and u_1 may vary severalfold. For example, when the jet diameter increases by 30%, the density of a monatomic vapor ($\gamma = 5/3$) falls by a factor of about 3, the temperature by a factor of 2.1, and the pressure by a factor of 6.2, whereas the velocity rises by a factor of 1.7 (the expansion is assumed to be adiabatic). However, even after this considerable reduction in the pressure, it is still higher than the atmospheric value $p_e = 1$ atm, because $p_1 = p_0/6.2 \approx 0.2 p_s(T)/6.2 \approx 0.034 p_s(T)$ and $p_s(T) \gtrsim 10^2$ atm. This means that the influence of the external pressure on the vapor flow in the region $x \lesssim d$ can usually be neglected (unless we are dealing with experiments at higher external pressures p_e).

We now have to allow for the possible interaction between the vapor jet and the laser beam penetrating it on the way to the target surface. At the vapor temperatures under consideration $T_v \sim T_{ev}^{(0)}$, corresponding to single ionization of the vapor atoms, the absorption of the optical radiation is due to the photoelectric and bremsstrahlung effects and the absorption coefficient μ_v is given by the Kramers–Unsöld formula (see, for example, [22] Chap. V, § 6):

$$\mu_v = \mu_0 e^{-\tilde{\Delta}/T}, \quad \mu_0 = \frac{8\pi}{3\sqrt{3}} \frac{e^6 N T_v}{hc(\hbar\omega)^3}, \tag{2.8}$$

where N is the density of atoms in the vapor, $\hbar\omega$ is the photon energy, c is the velocity of light, $\tilde{\Delta} = \Delta - \hbar\omega$, and Δ is the energy of single ionization of the vapor atoms. Near the target surface, where the vapor has not yet fully expanded ($x \ll d$), we have $N = j/Mc_0 = (1-R)I/q_1 c_0$, $T_v = T_0 + \beta_1 T$, and, consequently

$$NT_v = \beta_1 \frac{1-R}{\eta} \frac{I}{c_0}. \tag{b}$$

Hence, for metals and graphite [$(1-R)/\eta \approx 2 \times 10^2$, $c_0 = \sqrt{\beta_1 \gamma T/M} \approx (5-10) \times 10^4$ cm/sec] and $I \approx 10^6$ W/cm^2, we find that $NT_v \approx 0.15$–0.3 J/cm^3 and the pre-exponential factor μ_0 in Eq. (2.8) is always of the order of 10^3 cm^{-1} for $\hbar\omega \approx 1$ eV. However, since in this range of the vapor temperatures T_v and photon energies ($\hbar\omega \sim 1$ eV), we have $\tilde{\Delta}/T_{ev} \gg 1$, the absorption coefficient of the vapor μ_v is very small (for example, for a typical value of $\tilde{\Delta}/T_v \approx 30$, the coefficient is $\mu_v \sim 10^{-10}$ cm^{-1}). This estimate would seem to indicate that the vapor formed as a result of advanced evaporation of targets is so transparent that it cannot be heated to any significant degree by the laser radiation (particularly since away from the target surface the vapor temperature and density fall as a result of its expansion). However, the real situation is different: a "cold" vapor jet traveling from the target to meet the incident radiation may be "ignited" by a stable optical discharge in the same way as a cold jet in a gas burner. Moreover, the gas temperature rises behind the combustion front.

In fact, we can assume that in the vapor flow region under discussion ($x \lesssim d$) at some distance from the target surface a transverse hotter layer of optical thickness $\theta = \int \mu_v dx$ is established by some agency (for example, by the use of an external source, by analogy to a match used to light a gas burner). Existence of a layer of this optical thickness is clearly equivalent to the evolution of energy in this layer at a specific rate

$$Q = \frac{(1+Re^{-\theta})(1-e^{-\theta})}{j} I_0 = \frac{1+Re^{-\theta}}{1-R}(e^{\theta}-1)q; \tag{2.9}$$

here, we have used Eq. (2.1) with the substitution of $I = I_0 \exp(-\theta)$, where I_0 is the intensity of the radiation incident on the layer in question from the laser source side; it is also assumed that the lateral expansion of the jet is slight so that the vapor flux density j changes only slightly. If the specific heating rate Q is insufficient so that the velocity of the resultant detonation (more exactly, optical detonation) wave v_D (relative to the vapor) is less than the velocity u_1 of the arriving jet, such a layer cannot be maintained by the radiation and the vapor jet "blows it away." However, if $u_D > u_1$, this hotter vapor layer begins to expand in both directions because of the absorption of the laser radiation energy until the layer position becomes stable: this produces a steady-state optical discharge in the vapor jet. The discharge boundary facing the laser source is always located at the point where fast three-dimensional expansion of the vapor begins, i.e., at the distance $x \sim d$ from the target surface. The steady-state discharge layer thickness Δx and the vapor temperature in this layer T_2 [and, therefore, the optical thickness $\theta \approx \mu_v(T_2)\Delta x$] are governed by the specific heating rate $Q = Q(T_2, \Delta x)$, given by Eq. (2.9), which must be such as to ensure that the detonation wave velocity is equal to the velocity $u_1 = u_1(x)$ of the "cold" vapor arriving from the target, i.e.,[4)]

$$u_1(x) = v_D(Q), \tag{2.10a}$$

and, moreover, the heating rate must ensure that the

[4)] It should be noted that the existence of an optical discharge has no influence on the distribution of the hydrodynamic parameters of the vapor along the x axis [and, in particular, the velocity $u_1(x)$] ahead of the vapor front because its flow is supersonic ($u_1 > c_1$).

gas velocity behind the detonation front $u_2(Q)$ is equal to the velocity of sound $c_2=\sqrt{\gamma T_2/M}$ (Chapman–Jouguet rule), i.e.,

$$T_2=\frac{M}{\gamma}u_2^2(Q). \qquad (2.10b)$$

The feedback mechanism ensuring the stability of an optical discharge in our case is as follows: an accidential increase in the optical thickness of the discharge above its steady-state value θ reduces the radiation intensity $I=I_0\exp(-\theta)$ on the target surface, which always reduces the vapor flux density j [see Eq. (2.1)] and its initial temperature $T_0=\beta_2 T$ [see Eq. (2.7)] and, consequently, it reduces the absorption coefficient of the vapor μ_v, i.e., the optical thickness of the layer. Conversely, when θ falls accidentally, the vapor density and its temperature T_0 increases, the absorption coefficient μ_v also increases, and the optical thickness returns to its steady-state value.

We can use Eqs. (2.10a) and (2.10b) to find the discharge temperature T_2 and the thickness of the steady-state discharge layer Δx only if we know the dependence of the velocity u_1 on the coordinate x. Determination of this dependence is a separate hydrodynamic problem. However, if we are interested only in the discharge temperature T_2, there is no pressing need to find this dependence because, as will be shown immediately, T_2 depends only logarithmically on Δx and, therefore, we can quite accurately assume that $\Delta x\approx d$. Then, Eq. (2.10a) becomes redundant. Equation (2.10b) can be simplified, again with logarithmic precision, if we substitute $u_2=\gamma\sqrt{2(\gamma-1)Q/(\gamma+1)}$, i.e, we assume that the detonation wave is always strong.[5)] Then, according to Eq. (2.9), we find that the steady-state value of the optical thickness can be described approximately by

$$\theta=\frac{\gamma+1}{2\gamma(\gamma-1)}\frac{1-R}{1+R}\frac{\tilde{\Delta}}{q_1}\frac{T_2}{\tilde{\Delta}}\left[1-\frac{\gamma+1}{4\gamma(\gamma-1)}\left(\frac{1-R}{1+R}\right)^2\frac{\tilde{\Delta}}{q_1}\frac{T_2}{\tilde{\Delta}}\right], \qquad (2.11)$$

and the temperature T_2 can be found, in accordance with Eq. (2.8), from the equation $\tilde{\Delta}/T_2=\ln(\theta_0/\theta)$, where $\theta_0=\mu_0\Delta x\approx\mu_0 d$. An approximate solution of this equation is

$$T_2=\tilde{\Delta}/\Lambda,\quad \Lambda=\ln\left\{\frac{2\gamma(\gamma-1)}{\gamma+1}\frac{1+R}{1-R}\frac{q_1}{\tilde{\Delta}}\theta_0\ln\left[\frac{2\gamma(\gamma-1)}{\gamma+1}\frac{1+R}{1-R}\frac{q_1}{\tilde{\Delta}}\theta_0\right]\right\}. \qquad (2.12)$$

The value of the logarithm Λ is practically independent of the thermal properties of the target material and of the incident radiation intensity I, and is always very close to 10 (for $\theta_0=\mu_0 d\sim 10^3$–$10^4$, the values of Λ lie within the range 9–11).

Thus, the steady-state temperature T of the target surface being evaporated is always governed basically by its heat of evaporation q_1 [see Eq. (2.7)], whereas the vapor temperature $T_v=T_2$ near the surface ($x\lesssim d$) is basically governed always by the ionization energy of the vapor particles Δ (reduced by the photon energy $\hbar\omega$) and in most cases it is much higher than the temperature of the surface T. The heated vapor jet is separated from the colder target surface by a "cold" vapor layer which is in supersonic motion. According to Eqs. (2.11) and (2.12), the optical thickness θ of this jet is always $\sim\Lambda^{-1}$, i.e., it remains small compared with unity. It means that there is no significant screening of the target by the vapor.

We shall now demonstrate that in the case of metals (with the exception of such refractory materials as tungsten and molybdenum) and graphite the vapor temperature T_2 exceeds the target temperature by a factor of 2.5–4.5. We shall do this by transforming Eq. (2.12) to an expression of the type $T_2/T_{ev}=(\tilde{\Delta}/q_1)(q_1/T_{ev})/\Lambda$. In the case of metals (with the exception of tungsten and molybdenum) and optical-frequency radiation ($\hbar\omega\approx 1$ eV), we have $\tilde{\Delta}/q_1=2$–3, whereas $\eta=q_1/T_{bp}^{(0)}\approx 12$–$15$; hence, we find that $T_2/T_{bp}^{(0)}\approx 2.5$–$4.5$. For graphite, the corresponding ratio is $\tilde{\Delta}/q_1\approx 0.65$, but $q_1/T_{sbl}^{(0)}\approx 46$, therefore, $T_2/T_{sbl}^{(0)}\approx 3$ and the vapor temperature is $T_2\approx 12000$ °K. In the case of tungsten and molybdenum we have, respectively, $\tilde{\Delta}/q_1\approx 0.75$, $q_1/T_{bp}^{(0)}\approx 17.5$ and $\tilde{\Delta}/q_1\approx 0.9$, $q_1/T_{bp}^{(0)}\approx 15.5$; we thus find that in the case of these two metals $T_2/T_{bp}^{(0)}\approx 1.3$, i.e., the temperature T_2 exceeds the target surface temperature T only slightly (if at all).

The steady-state heating of the vapor by radiation was first noted in[4,23]. A direct (spectroscopic) determination of the temperature T_2 during quasicontinuous irradiation ($\tau\sim 10^{-3}$ sec, $\lambda=1.06$ μ, $I\sim 10^7$ W/cm^2) was first reported in[24] (for bismuth and aluminum). The results of these measurements were in good agreement with the above theoretical conclusions on the degree of heating of the vapor. These experiments also showed that the appearance of an optical discharge in vapors was spontaneous, i.e., that it resulted from fluctuations. This is an important point in the theory of laser jet engines. The importance of the existence of a steady-state heated vapor layer will become clearer later (see Sec. 2b).

The advanced evaporation and the steady-state heating of the vapor near the target surface ($x\lesssim d$) described above occur as long as the radiation intensity is not too high, so that an electron avalanche does not develop in the vapor, i.e., as long as a "laser spark" does not appear in the vapor (see[20]). In the evaporation mechanism of thrust in a laser jet engine this effect should naturally be avoided because it results in strong plasma screening of the target (propellant) from the incident

---

[5)] In general, the velocity of a gas behind the front of a detonation wave is (see[21] §120)

$$u_2=\gamma\sqrt{\frac{2(\gamma-1)Q}{\gamma+1}}\left(\frac{\gamma-1}{2\gamma}+\frac{\gamma+1}{2\gamma}\sqrt{1+\frac{2c_1^2}{(\gamma^2-1)Q}}\right)$$

($c_1=\sqrt{\gamma T_1/M}$ is the velocity of sound ahead of the detonation wave front). In the case of a strong wave, when $(\gamma^2-1)Q\gg c_1^2$, we then obtain the formula for u_2 quoted in the text. If $(\gamma^2-1)Q\sim c_1^2$, this formula gives only the order of magnitude of u_2, which—as shown later—is quite sufficient for the determination of T_2. The case $(\gamma^2-1)Q\ll c_1^2$ is excluded from the consideration of the steady-state regime because then the velocity of the detonation wave is $v_D\propto c_1<u_1$.

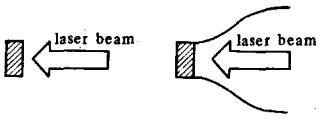

FIG. 1.

radiation, which stops the evaporation.[6] If the irradiation is continuous, the target evaporation becomes pulsating and the laser beam power is not used efficiently.

Consequently, the pure evaporation mechanism (i.e., the mechanism which is not interrupted by laser sparks in the vapor) can be obtained only if the intensity I of the radiation incident on a target lies within the range $I_{ev} < I < I_{aval}$, where I_{aval} is the threshold of the development of an electron avalanche (spark) in the vapor. This pure evaporation mechanism can readily be achieved in the visible and near infrared range. This is due to the fact that in this frequency range the value of I_{aval} is usually several orders of magnitude higher than I_{ev}. This is confirmed by the experimental results and is readily supported by the following theoretical estimates. An electron avalanche develops in a vapor (see[20]) if the rate of increase of the energy of free electrons in the vapor due to the inverse bremsstrahlung $(\delta\varepsilon/\delta t)_E = 4\pi e^2 I \nu_{eff}/mc\omega^2$ (e and m are the electron charge and mass, and ν_{eff} is the effective frequency of collisions between electrons and vapor particles, governed by the transport scattering cross section[7]) at least exceeds the maximum rate of energy losses suffered by electrons because of elastic collisions with the vapor particles $(\delta\varepsilon/\delta t)_{el} \approx (2m/M)\nu_{eff}\Delta$. Hence, we obtain the lower limit of I_{aval}:

$$I_{aval} > 6\cdot 10^9 \frac{\Delta\ (\text{eV})}{\lambda^2(\mu)A}\ (\text{W/cm}^2), \qquad (2.13)$$

where A is the atomic weight and $\lambda = 2\pi c/\omega$ is the wavelength of the incident radiation. For the majority of simple substances (and, in particular, in the case of metals) we have $\Delta(\text{eV})/A > 0.03$ (for graphite, 0.09). Therefore, if $\lambda \approx 1\mu$, $I_{aval} > 2\times 10^8$ W/cm^2, whereas the advanced evaporation threshold is $I_{ev} \sim 10^5$–10^6 W/cm^2 (as given above).

In the far infrared range (in particular, in the case of CO_2 laser radiation of $\lambda = 10.6\mu$ wavelength), the evaporation I_{ev} and electron avalanche I_{aval} thresholds may be so close that it will be difficult or impossible to realize the pure evaporation mechanism (for details see[12] and Sec. 3 in the present paper).

Thus, the evaporation mechanism of thrust (during continuous irradiation) can be realized effectively only in the visible and near infrared range, where we can readily avoid the appearance of an optical breakdown (spark) in the vapor.[8] We shall now consider in detail the main characteristics of the evaporation mechansim of thrust.

B. Principal characteristics of evaporation reactive thrust mechanism

We shall now consider two types of target (nozzle): a plane target alone and a plane target with an expanding nozzle (Fig. 1). The first type of target (Fig. 1a) can be regarded as the limiting case of a Laval nozzle with maximum under expansion; the second type (Fig. 1b) can be treated as an ordinary Laval nozzle, which we shall regard as calculated.[9] For both types of target the steady-state thrust force F is given by the well-known formula

$$F = Gu_e; \qquad (2.14)$$

here, $G_0 = Sj = S(1-R)I_0\exp(-\theta)/q$ is the rate of consumption of the propellant (S is the target area equal to the laser beam area); this expression is derived using Eq. (2.1) and u_e is the velocity of the vapor at the nozzle edge. In the case of a plane target without a nozzle, we have $u_e = c_0 = \sqrt{\gamma T_0/M} = \sqrt{\beta_1\gamma T/M}$, i.e., the vapor velocity is governed by the target surface temperature T (see Sec. 2A); the additional heating of the vapor by the radiation in the region $x \lesssim d$ thus has no influence on the velocity u_e and, consequently, it does not affect the thrust force F. An expanding nozzle allows us to heat the vapor additionally so as to increase the thrust force. The part of the nozzle located beyond the detonation wave front (at a distance $x \approx d$ from the target surface) can be regarded as the throat section. In this section the velocity of flow of the vapor is equal to the local velocity of sound $c_2 = \sqrt{\gamma T_2/M}$ (Chapman–Jouguet rule). A fast adiabatic expansion of the vapor in the expanding nozzle begins beyond this section. The vapor velocity u_e at the edge of the nozzle, where the pressure is equal to the external pressure of the ambient gas (air) p_e, is given by the well-known relation which follows from the Bernoulli equations and from the Poisson adiabat (see, for example,[25]):

$$u_e = \sqrt{\frac{\gamma+1}{\gamma-1}}c_2\sqrt{1-\frac{2}{\gamma+1}\left(\frac{p_e}{p_2}\right)^{(\gamma-1)/\gamma}}, \qquad (2.15)$$

where p_2 is the vapor pressure in the throat section (behind the detonation wave front at $x \approx d$). Since the lateral expansion of the vapor in the region $x \lesssim d$ is slight, it follows from the law of conservation of the vapor momentum that the pressure is $p_2 \approx p_0 = \beta_2 p_s(T)$ (see Sec. 2A) or, if we use the relationship $j(T) = \alpha j_{vac}(T)$ and Eqs. (2.1) and (2.2),

$$p_2 = \frac{2\pi\beta_2}{\alpha}\frac{1-R}{1-r}\frac{I_0 e^{-\theta}}{q}\bar{v}_1(T), \quad \bar{v}_1(T) = \sqrt{\frac{T}{2\pi M}}. \qquad (2.16)$$

We shall denote the values of the velocity u_e for the targets without and with a nozzle by $(u_e)_I$ and $(u_e)_{II}$. The ratio of these velocities is

[6] If the target is in air, a spark may initiate an optical detonation wave traveling opposite to the laser beam (see[12]).

[7] Our expression for $(\delta\varepsilon/\delta t)_E$ is valid if $\omega^2 \gg \nu_{eff}$, which is obeyed in the situation discussed above right up to the far infrared range.

[8] Although formally even in the near ultraviolet range the photon energy is $\hbar\omega < \Delta$ and the one-photon photoelectric effect is still impossible in the vapor.

[9] The main concepts and terminology of jet engines can be found in, for example,[25].

$$\frac{(u_e)_{II}}{(u_e)_I}=\sqrt{\frac{\gamma+1}{\beta_1(\gamma-1)}}\sqrt{\frac{T_2}{T}}\sqrt{1-\frac{2}{\gamma+1}\left(\frac{p_e}{p_2}\right)^{(\gamma-1)/\gamma}}. \quad (2.17a)$$

In the case of a monatomic vapor ($\gamma=5/3$) heated to $T_2/T\approx 3$, we find (assuming that $\beta_1\approx 0.65$)

$$\frac{(u_e)_{II}}{(u_e)_I}\approx 4.3\left[1-\frac{3}{4}\left(\frac{p_e}{p_2}\right)^{2/5}\right]^{1/2}. \quad (2.17b)$$

Under typical experimental conditions ($I_0\approx 3\times10^6$ W/cm^2, $q\approx 10^4$ J/g), it follows from Eq. (2.16) and the experimental results that the pressure is $p_2\approx 10$–30 atm. Assuming that $p_2=20$ atm, we find that if $p_e=1$ atm, then $(u_e)_{II}/(u_e)_I\approx 3.8$, whereas for $p_e=0.1$ atm, this ratio is ≈ 4.1.

Thus, the use of a nozzle ensuring the calculated flow regime should increase (other conditions being constant) the thrust force F by a factor of about 4. The vapor flow velocity $(u_e)_{II}$ can be estimated from $(u_e)_{II}\approx 4\sqrt{\beta_1\gamma T/M}\approx\sqrt{16\beta_1\gamma q/\eta}$, where for metals characterized by $\eta=12$–15 we have $\sqrt{16\beta_1\gamma/\eta}\approx 1$ and, therefore, $(u_e)_{II}\approx\sqrt{q}$, whereas for graphite characterized by $\eta\approx 46$ we have $\sqrt{16\beta_1\gamma/\eta}\approx 1/\sqrt{3}$ and, therefore, $(u_e)_{II}\approx\sqrt{q/3}\approx 6$ km/sec if $q\approx 1.2\times10^5$ J/g.

One of the most important characteristics of laser jet engines, which governs the possibility of their construction and use, is the scale factor, defined as the ratio of the laser beam power $P_0=SI_0$ needed to produce a given thrust force F. It follows from Eq. (2.14) that this scale factor is

$$\frac{P_0}{F}=\frac{e^\theta}{1-R}\frac{q}{u_e}. \quad (2.18)$$

Hence, we can see that the nozzle reduces almost fourfold the scale factor. Since in all cases we an assume approximately that $u_e\propto\sqrt{q}$, it follows from Eq. (2.18) that $P_0/F\propto\sqrt{q}$.

This means that the minimum scale factor is obtained if easily vaporized substances are used as targets. Substituting in Eq. (2.18) the velocity $u_e=(u_e)_{II}\approx\sqrt{q}$ and $e^\theta/(1-R)\approx 2$ (this applies, for example, to bismuth), we obtain the following estimate

$$\frac{P_0}{F}\approx 0.6\sqrt{q}\ \text{(kW/kgf)},$$

where q is given in joules per gram. For $q\approx 10^3$ J/g the scale factor is $(P_0/F)\approx 20$ kW/kgf. This scale factor, corresponding to relatively easily vaporized substances, is of the same order as that attained at present in the best variants of electroreactive rockets and is slightly less than the values that are obtained under optimal conditions for ordinary jet engines with chemical fuel if the value of P_0 is understood to be the thermal power evolved in the combustion chamber (see Table on p. 126 in[25]).

In the case of graphite $[(u_e)_{II}\approx\sqrt{q/3},\ e^\theta(1-R)\approx 1]$, Eq. (2.18) gives $(P_0/F)\approx 190$ kW/kgf.

Easily vaporized substances, which are desirable in order to minimize the scale factor, are undesirable from the point of view of another important characteristic of jet engines, which is the specific impulse F_{sp}, equal to the ratio of the thrust force F to the rate of consumption of the propellant mass gG (g is the acceleration due to gravity). According to Eq. (2.14), $F_{sp}=F/gG=u_e/g$ and, consequently, it depends in the same way on the specific heat of evaporation as the ratio of the laser power to the thrust obtained: $F_{sp}\propto\sqrt{q}$.

Thus, difficult-to-vaporize substances should be used to obtain the maximum specific impulse. One of such substances is graphite for which $q\approx 1.2\times10^5$ J/g and $(u_e)_{II}\approx\sqrt{q/3}\approx 6$ km/sec, which exceeds the maximum velocity of flow in the most efficient two-component chemical fuel of the oxygen–hydrogen type ($u_{max}=5.2$ km/sec). The specific impulse is then $F_{sp}\approx 600$ sec, which exceeds the specific impulse obtained in jet engines with a conventional chemical fuel (for example, it is twice the specific impulse of the Vostok launch rocket and 2.2 times the specific impulse of the Saturn-5 launch rocket) but is less than the specific impulse achieved in current electroreactive rockets.

Finally, we shall consider another characteristic of laser jet engines with the evaporation thrust mechanism, which is the efficiency of conversion of the laser power into the useful (thrust) kinetic energy flux in the vapor. This is known as the power conversion efficiency and is denoted by η_F:

$$\eta_F=\frac{Gu_e^2}{2P_0}=\frac{1-R}{2e^\theta}\frac{u_e^2}{q}. \quad (2.19)$$

It is clear from the above formula that the efficiency η_F is completely independent of the specific heat of evaporation and in the case of a laser jet engine with a nozzle it amounts to 20–30%.

These estimates of the characteristics P_0/F, F/gG, and η_F are given for a device with a nozzle and they are correspondingly poorer for a laser jet engine without a nozzle: P_0/F increases by a factor of 4 and F/gG decreases by the same factor, where η_F decreases by a factor of about 15. These "poorer" values should be compared with the known experimental data all of which have been obtained for plane targets (see[2,4,5,7]). The experimental values of P_0/F and F/gG are in good agreement with the above estimates.

3. LASER AIR-BREATHING JET ENGINE

In the realization of the basic idea of a laser air-breathing jet engine, which is the use of laser radiation in heating the atmospheric air reaching the engine, it is necessary to ensure that the intensity of the radiation in the heated zone is sufficiently high and that the air is characterized by a strong (nonlinear) absorption with an effective photon path not exceeding the dimensions of the heated zone. On the other hand, the intensity of the laser beam traveling through the atmosphere should be less than the nonlinear absorption threshold. This means, in particular, that such an air-breathing engine should always include a device for focusing of the laser beam.

The required strong absorption laser radiation inside a heated zone can only be achieved by the formation and maintenance throughout the irradiation period of an

optical discharge in the air in this region. There are several ways in which optical discharges in gases can be made self-sustaining[20] but not all of them can be used efficiently and stably in an air-breathing engine. We shall consider only the specific variant of this engine which we investigated both theoretically and experimentally.[8] The physical basis of this investigation was given in our earlier papers[9,12] dealing with the low-threshold breakdown of gases near solid targets by CO_2 laser radiation.

In the variant under consideration a laser air-breathing jet engine is operated in the pulse-periodic (pulsating) regime because of the corresponding nature of the laser emission ("pulsejet concept"). Each radiation pulse is assumed to cross the atmosphere without significant absorption and to reach a parabolic reflector which is in the rear part of a flight vehicle and is attached rigidly to this vehicle. The pulse radiation intensity reaching the reflecting surface should be below the damage threshold (in particular, below the evaporation threshold) of the reflector material but sufficient to exceed the optical breakdown threshold of the air in the focal region of the reflector. This main condition is easiest to satisfy by the use of CO_2 lasers (or other lasers emitting in the far infrared range when these are developed with the necessary average output power and a sufficiently high efficiency). This preference follows from the fact that the breakdown threshold of air (and of gases in general) can be reduced quite considerably in the far infrared by placing in the focal region an auxiliary solid target which initiates the low-threshold breakdown.[9,12] At atmospheric pressure the breakdown threshold of air at $\lambda = 10.6\mu$ falls to 10^6–10^7 W/cm^2 for pulse durations $\tau \sim 10^{-5}$–10^{-6} sec, i.e., it is 2–3 orders of magnitude less than the breakdown threshold of pure air in the absence of such a target. The physical explanation of this effect is given in[12]. The point is that initially the breakdown (electron avalanche) develops in a dense vapor which appears near the target surface as a result of its evaporation (or, more exactly, as a result of the evaporation of its surface layer whose physicochemical composition may differ considerably from the target material itself) under the action of the leading part of a laser pulse. This is why the CO_2 laser radiation (and, in general, long-wavelength radiation) is preferred (see the paragraphs in Sec. 2A dealing with the optical breakdown-spark formation-in a vapor). According to Eq. (2.13), the lower limit of the threshold intensity I_{aval} at $\lambda = 10.6\mu$ is $I_{aval} > 5.4 \times 10^7 \Delta$ (eV)/A W/cm^2. It is shown in[12] that in the case of atomic vapor this lower limit is close to the true value of the breakdown threshold which, in its turn, is usually close to the target evaporation threshold (see Sec. 2A).

Breakdown (a spark) in the vapor causes the region of strong absorption to expand rapidly to the surrounding air (by heating and ionization) and, therefore, optical breakdown of air occurs in the focal region giving rise to an explosion in which a large part of the laser pulse energy is evolved. This explosion in the focal region excites a shock wave in the surrounding cold air and this shock wave presses on the reflector which thus acts also as a pressure plate. If before the arrival of the next laser pulse the region inside the reflector is refilled with cold air with the initial parameters, pulse-periodic irradiation should produce a sequence of shock waves with an average thrust $F_{av} = J/\tau_1$, where J is the total mechanical impulse transferred to the flight vehicle by one shock wave and τ_1 is the repetition period of the radiation pulses.

We shall now consider the selection of the optimal values of the laser pulse duration τ and repetition period τ_1. The pulse duration τ should be sufficiently long to ensure that the optical breakdown of air takes place and a major part of the laser pulse energy E is absorbed in the breakdown plasma. The breakdown development time in the case of CO_2 laser radiation intensities $I \sim 10^7$ W/cm^2 is $\sim 10^{-6}$ sec (see[12]). Consequently, it is necessary to satisfy the condition $\tau \gtrsim 10^{-6}$ sec. On the other hand, τ should be sufficiently short so that during the pulse the shock-wave front does not travel too far away from the center of the explosion, i.e., it should satisfy the condition $\tau \ll R/v_{sw}$, where R is the focal length of the reflector and v_{sw} is the velocity of a shock wave in air, which depends on the amount of energy supplied to the explosion E_1: $v_{sw} \propto (E_1/\rho R^3)^{1/2}$ (ρ is the density of cold air). Thus, we must satisfy the condition $\tau \ll (\rho R^5/E_1)^{1/2}$. We shall show later that under optimal operating conditions in a laser air-breathing jet engine we should have $R/(E_1/p_e)^{1/2} \lesssim 1/2$ (p_e is the external pressure of air). Hence, we obtain the final estimate of the upper limit to the pulse duration:

$$\tau \ll \frac{\rho^{1/2} E_1^{1/3}}{2^{5/2} p_e^{5/6}}. \qquad (3.1)$$

On the basis of Eq. (3.1) and with $p_e = 1$ atm, we obtain: if $E_1 \sim 1$ J, then $\tau \ll 10^{-5}$ sec, i.e., the optimal value is $\tau_{opt} \sim 10^{-6}$ sec; if $E_1 \sim 10^3$ J, then $\tau_1 \ll 10^{-4}$ sec, i.e., τ_{opt} lies within the range 10^{-5}–10^{-6} sec.

The repetition period of laser pulses τ_1 should, on the one hand, exceed the time needed to fill the space inside the reflector, (which also acts as the pressure plate) with cold air which has the necessary initial parameters. This time is of the order of D/c_a, where D is a characteristic dimesion of the reflector and c_a is the velocity of sound in cold air. If $D \approx 30$ cm, we find that $\tau_1 > 10^{-3}$ sec. On the other hand, in practical systems the pulse repetition frequency $1/\tau_1$ should be sufficiently high to ensure the necessary average laser beam power $P_{av} = (\tau/\tau_1) S I_0$. In numerical estimates we may assume that the optimal off-duty factor is $\tau_1/\tau \sim 3 \times 10^2$ (when the pulse repetition frequency is $1/\tau_1 \approx 300$ Hz and the pulse duration is $\tau \approx 10^{-5}$ sec) and that the average power P_{av} represents 0.3% of the pulse power SI_0.

We shall now turn to the more complex problem of the optimal position of the center of the explosion, i.e., of the position of the focal region relative to the reflector surface. We shall first consider this problem qualitatively. It follows from general considerations that the average thrust force is $F_{av} = G_{av} u$, where G_{av} is the average consumption of air per period and u is some effective velocity of flow of the hot air. At this stage we can ignore the counterpressure of the surrounding

air so that we have $G_{av} \sim \rho R^3/\tau_1$ and $u \sim v_{sw} \sim \sqrt{E_1/\rho R^3}$. Hence, we obtain

$$F_{av} \sim \frac{\rho R^3}{\tau_1}\left(\frac{E_1}{\rho R^3}\right)^{1/2} = \left(\frac{\rho}{p_e}\right)^{1/2}\left(\frac{R}{R_0}\right)^{3/2} P_{av}, \qquad (3.2)$$

where $P_{av} = E_1/\tau_1$ and $R_0 = (E_1/p_e)^{1/3}$ is the characteristic dynamic length. It follows from Eq. (3.2) that the ratio of the laser power to the thrust obtained, i.e., the scale factor, is $P_{av}/F_{av} \propto (R/R_0)^{-3/2}$, so that the scale factor decreases when the parameter R/R_0 is increased. However, this formula is valid only if $R/R_0 \ll 1$, when the counterpressure is unimportant. If $R/R_0 > 1$, the counterpressure is important and a shock wave reaching the reflector (pressure plate) is weakened so that the scale factor begins to rise again. A minimum should be observed at $R/R_0 \sim 1$, which corresponds to the optimal (from the point of view of the thrust force) operation of a laser air-breathing jet engine.

A more rigorous analysis including allowance for the counterpressure can be made using the theory of point explosions. The total pressure impulse J transferred by a shock wave to an axisymmetric surface (when the center of the explosion is located on the axis of this surface) can be deduced by dimensional analysis in the form (see p. 279 in[26]):

$$J = \sqrt{\frac{\rho E_1}{R}}\, D^2 f\left(\frac{R}{D}; \frac{R}{R_0}\right); \qquad (3.3)$$

here, E_1 is the energy evolved at the center of the explosion; in our case we have $E_1 = \alpha E$, where E is the laser pulse energy and α is the efficiency of energy transfer found experimentally. Our experiments (see Fig. 3 later) demonstrated that in the case of sufficiently high values of E the value of α tends to unity. The other notation used above is as follows: ρ is the density of the cold air in the space adjoining the internal side of the reflecting surface and it should be noted that this density need not be equal to the external density of air ρ_e; R is the distance of the center of the explosion from the vertex of the reflecting surface, which—in our case—is the focal length of the parabolic reflector; D is the characteristic transverse dimension of the reflecting surface, which is the paraboloid diameter; f is the dimensionless function of the geometric parameter R/D and the dynamic parameter R/R_0.

Equation (3.3) can be used to obtain a more general expression for the ratio of the laser power to the thrust force P_{av}/F_{av}. If we assume that the efficiency of energy transfer is close to unity, i.e., if $E_1 \approx E$, we find that

$$\frac{P_{av}}{F_{av}} \approx \frac{E_1}{J} = \frac{c_a\sqrt{\rho_e/\rho}}{(R/R_0)^{3/2} f_1(R/D;\, R/R_0)}, \qquad (3.4)$$

where $c_a = \sqrt{\gamma p_e/\rho_e}$ is the velocity of sound in air; the dimensionless function is $f_1 = \sqrt{\gamma} f (R/D)^2$. The formula (3.4) yields the conditions for the dynamic similarity of the ratio of the laser power to the thrust developed in a laser air-breathing jet engine:

$$\frac{R}{D} = \text{const}, \quad \frac{R}{(E_1/p_e)^{1/3}} = \text{const}. \qquad (3.5)$$

In the geometrically similar case (R/D = const), these conditions are satisfied if the energy input per pulse is $E = \text{const} \cdot p_e R^3$.

The dependences of the functions f and f_1 on the ratio R/R_0 describe the influence of the counterpressure of the surrounding air; this pressure increases with the value of R/R_0. Therefore, for a given value of the parameter R/D, an increase in R/R_0 results in a monotonic fall of the functions f and f_1. Hence, it follows from Eq. (3.4) that the ratio of the laser power to the thrust P_{av}/F_{av} has a minimum at some optimal value $(R/R_0)_{opt}$; this optimal value $(R/R_0)_{opt}$ and the corresponding minimum ratio of the laser power to the thrust depend on R/D. This dependence can be obtained approximately from the following considerations.

The optimality condition is clearly equivalent to the calculated nozzle condition, i.e., in the present case the pressure at the points on the reflector furthest from the focus is most of the time equal to the external pressure p_e. Numerical calculations dealing with point explosions allowing for the counterpressure (see pp. 273–274 in[26]) enable us to rewrite the above optimality condition in the form

$$\frac{R_{max}}{R_0} \approx \frac{1}{2} \quad \text{or} \quad \left(\frac{R}{R_0}\right)_{opt} \approx \frac{1/2}{R_{max}/R}. \qquad (3.6)$$

where R_{max} is the greatest distance of the points on the surface of the reflector from the focus. In the case of axisymmetric surfaces the ratio R_{max}/R can always be expressed in terms of the geometric parameter R/D. If the condition of Eq. (3.6) is satisfied, the pressure in the shock-wave front is $p_{sw} \approx 3p_e$, whereas the pressure behind this front rapidly reaches a steady value of $0.35p_{sw} \approx p$, i.e., it rapidly falls to the external pressure.

In the case of a parabolic surface of interest to us, we have $R_{max} = R + L = R[1 + (D^2/16R^2)]$ (L is the length of the paraboloid) and it follows from Eq. (3.6) that

$$\left(\frac{R}{R_0}\right)_{opt} \approx \frac{1/2}{1 + (D/4R)^2}. \qquad (3.7)$$

Hence, we can see that $(R/R_0)_{opt} \lesssim 1/2$, which we have used above in deriving the condition (3.1).

In those cases when the dynamic length R_0 is given (i.e., when the energy input E_1 and the external pressure p_e are given), the optimal ratio $(R/R_0)_{opt}$ corresponds to the optimal focal length R_{opt}. Then, Eq. (3.7) allows us to find R_{opt} as a function of the diameter D if we substitute $R = R_{opt}$. Solving this equation, we obtain

$$R_{opt} \approx \frac{R_0}{4}\left[1 - \sqrt{1 - \left(\frac{D}{R_0}\right)^2}\right]. \qquad (3.8)$$

Hence, it is clear, firstly, that for a given value of R_0 the optimum (i.e., the "calculated nozzle") exists only in the range of diameters $0 \leq D \leq R_0$. It also follows from Eq. (3.8) that the length of the paraboloid corresponding to the optimal focus is $L_{opt} = D^2/16R_{opt} \geq R_{opt}$ (this follows when we take the equality sign in the above range so that $D = D_{max} = R_0$). It means that, for a given

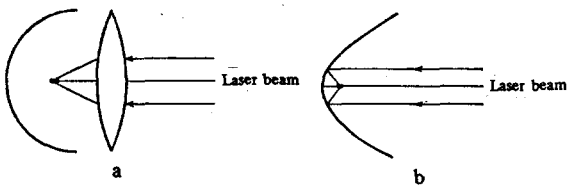

FIG. 2.

R_0, the optimal focus is always inside the paraboloid (or on its axis for $D = D_{max} = R_0$).

We shall also note that the existence of a maximum calculated diameter $D_{max} = R_0$ implies that the minimum pulse intensity over the aperture of the calculated reflector is (it is assumed that $\alpha = 1$)

$$I = \frac{4E}{\pi\tau D_{max}^2} = \frac{4p_e^{2/3}E^{1/3}}{\pi\tau} \approx 2.7 \cdot 10^6 E^{1/3} \text{ (W/cm}^2\text{)}. \qquad (3.9)$$

This estimate applies to the case $\tau = 10^{-5}$ sec, $p_e = 1$ atm, and E is expressed in joules. If we assume that the maximum intensity I reaching the reflector surface is 10^6 W/cm^2, it follows from Eq. (3.9) that the maximum laser pulse energy E at which we can still use the "calculated (theoretical) reflector" is approximately 50 kJ; then, $D_{max} = (E/p_e)^{1/3} \approx 80$ cm.

The above method of obtaining the dependence of the optimal ratio $(R/R_0)_{opt}$ on the geometric parameter R/D does not give us the corresponding value of the minimum ratio of the laser power to the thrust P_{av}/F_{av}. This ratio can be found only if we know the function $f_1(R/D; R/R_0)$ which occurs in Eq. (3.4). A theoretical determination of this function is quite difficult but it can be found numerically. It should also be noted that in obtaining the minimum value of the ratio of the laser power to the thrust we are ignoring the dependence of the resistance of air on the geometric shape of the flight vehicle. Clearly, such allowance is essential in optimization of the total force acting on the flight vehicle.

We carried out experiments in which we determined that the absolute values of the ratio of the laser power to the thrust P_{av}/F_{av} for various values of the parameter RR_0.[10] We used a CO_2 laser emitting pulses of $\tau \sim 10^{-6}$ sec duration. In the first series of experiments the pressure was received by hemispheres of diameters D which were varied from 4 to 15 cm. Radiation was focused by a lens approximately at the center of curvature of the hemisphere (Fig. 2a). The energy of the laser pulses was also varied up to $E \approx 50$ J. In all cases the breakdown of air at the focus occurred without any initiation.

First, we determined the energy transfer efficiency $\alpha = E_1/E$. Two graphite calorimeters were used in measuring the energy E reaching the focusing lens and

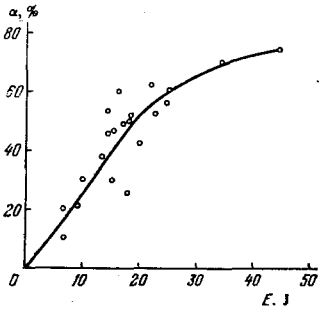

FIG. 3.

the energy E_T transmitted by the breakdown plasma (in this case the hemisphere was moved out of the beam). The values of the efficiency $\alpha = (E - E_T)/E$ were determined as a function of E (Fig. 3). We found that an increase in the incident energy E increased the efficiency α and at the maximum energies used in our experiments ($E \approx 50$ J), the efficiency reached about 75%.

The total mechanical impulse J transmitted to the surface (pressure receiver) by a shock wave created in optical breakdown was deduced from a deflection of a ballistic pendulum, whose "lens" was the hemisphere itself. We obtained numerous experimental values of the ratio J/E_1 (reciprocal of the scale factor known as the coupling coefficient) as a function of the dynamic parameter R/R_0 (Fig. 4a), where $R = D/2$ was the radius of this hemisphere.

As expected from theoretical ideas (discussed above), at some particular value of $R/R_0 = (R/R_0)_{opt}$ the coupling coefficient J/E_1 had a maximum (the scale factor or the ratio of the laser power to the thrust P_{av}/F_{av} had a minimum). In our experiments on a hemisphere we found that $(R/R_0)_{opt} \approx 1.5$; in this case the maximum value of the coupling coefficient was $(J/E_1)_{max} \approx 20$ dyn · sec · J^{-1}, which corresponded to the minimum value of the scale factor $P_{av}/F_{av} \approx 50$ kW/kgf.

In a second series of experiments the pressure receiver was a parabolic surface with a geometric pa-

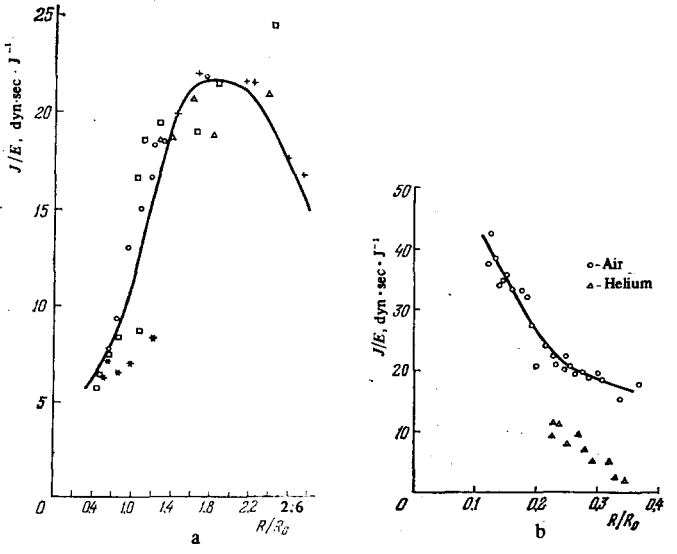

FIG. 4.

[10] These experiments were carried out under the direction of A. I. Barchukov and the authros of the present paper by a team headed by V. I. Konov and comprising A. A. Lyubin, N. I. Chapliev, V. P. Ageev, A. S. Silenko, G. P. Kuz'min, and N. N. Kononov.

rameter $R/D=1/7$, which acted also as a focusing element (a lens was not used—see Fig. 2b). Optical breakdown of the gas (the experiments were carried out in air and in helium) again occurred always without initiating devices. The pressure impulse J was measured in a similar manner. The efficiency of energy transfer α was not determined in the second series.

Figure 4b gives the experimental values of J/E plotted as a function of the parameter R/R_0 (for air and helium). According to Eq. (3.7), if $R/D=1/7$, the optimal value of $(R/R_0)_{opt}$ for air is approximately 0.1. We were able to reach this value of R/R_0 and then the coupling coefficient J/E increased still further. Clearly, one should assume that the experimental value of $J/E \approx 45$ dyn·sec·J^{-1} obtained for $(R/R_0)\approx 0.1$ for air was close to its maximum value. The corresponding minimum value of the scale factor P_{av}/F_{av} was then approximately 22 kW/kgf, i.e., it was close to the scale factors estimated for the evaporation mechanism in the case of easily vaporizable targets ($q\approx 10^3$ J/g, see Sec. 2a) and also for the best variants of electroreactive rockets.

4. CONCLUSIONS

The idea of using a laser energy source located outside a flight vehicle in creating a reactive thrust is still in the laboratory stage. It is difficult to say definitely whether it will lead to real laser jet engines. This will depend primarily on future developments in high-power laser technology. We shall now estimate the necessary laser powers from the above results for the main characteristics of laser jet engines.

We shall first consider a laser jet engine with the evaporation thrust mechanism and estimate the specific laser power, i.e., the power P_0 necessary to accelerate the final mass of a flight vehicle M_k to its final velocity V_k. The length of the vehicle trajectory in which a laser jet engine can operate is limited by the divergence of the laser beam. Even in the case of the most optimistic estimates of the minimum divergence of high-power laser beams in the atmosphere, we cannot expect divergence angles smaller than 10^{-5} rad. Then, the maximum length of the active part of the trajectory H_{max} cannot exceed 100 km (when the diameter of the nozzle target is $D\sim 1$ m). This means that acceleration of a flight vehicle by a laser to the specified final velocity V_k would require sufficiently strong acceleration throughout the active part of the trajectory, including the initial section. The main interest clearly lies in the case when the initial acceleration is $a_0=F/M_0\gg g$ (M_0 is the initial mass of the flight vehicle). We shall assume that this condition is satisfied.

Using Eq. (2.19) and the Tsiolkovskiĭ formula

$$\frac{M_0}{M_k}=e^{V_k/u_e} \tag{4.1}$$

we find that the specific laser power is

$$\frac{P_0}{M_k}=\frac{a_0u_e}{2\eta_F}e^{V_k/u_e}=\frac{a_ku_e}{2\eta_F}, \tag{4.2}$$

where $a_k=a_0\exp(V_k/u_e)$ is the final acceleration (the thrust force is assumed to be constant). Hence, we can see that, for a given initial acceleration a_0 and power conversion efficiency η_F, the specific laser power is minimal when the propellant flow velocity is $u_e=V_k$. Since the velocity u_e depends on the specific heat of evaporation q, we find that a given final velocity V_k can be obtained for minimal specific power P_0/M_k if the propellant has a certain specific heat of evaporation q. When the calculated nozzle is used so that $u_e\approx\sqrt{q}$, the optimal heat of evaporation is $q_{opt}\approx V_k^2$. Thus, in launching a vehicle to an earth satellite orbit, when $V_k\gtrsim 8$ km/sec, the optimal heat of evaporation is $q_{opt}\gtrsim 10^5$ J/g, i.e., one has to use materials which are very difficult to evaporate. Even graphite, for which $u_e\approx\sqrt{q/3}\approx 6$ km/sec, is not an optimal material (but close to it).

It also follows from Eq. (4.2) that the specific power P_0/M_k increases with the final acceleration a_k. Near an optimum, when the velocity ratio V_k/u_e differs little from unity, the initial a_0 and final a_k accelerations may differ only severalfold and, therefore, in estimates we may assume that $a_k\sim V_k^2/H_{max}$. If $V_k\gtrsim 8$ km/sec and $H_{max}\gtrsim 100$ km, we find that $a_k\gtrsim 100g$; then, the specific power for graphite ($u_e\approx 6$ km/sec, $\eta_F\approx 0.3$), is $P_0/M_k\gtrsim 10^4$ W/g.

Consequently, in launching to a satellite orbit a vehicle with a final mass M_k+100 kg one would have to evaporate $M_0-M_k=M_k[\exp(V_k/u_e)-1]\approx 300$ kg of graphite by a laser beam of $P_0\gtrsim 10^9$ W power in $t\sim V_k/a_k\sim 10$ sec. A stationary laser unit with this power output would solve the problem of repeated use of power sources needed to inject light satellites into terrestrial orbits. However, it is very doubtful whether such a "superlaser" could be built at present.

The situation simplifies greatly if we consider the acceleration of smaller final masses M_k to lower velocities V_k by lower accelerations. For example, if $M_k=25$ kg, $V_k=1$ km/sec, and $a_0=25g$, the use of a propellant with the heat of evaporation $q_{opt}\approx 10^3$ J/g requires a laser power of $P_0\approx 10^7$ W; then, the mass of the "propellant" is 43 kg and the acceleration time (laser operation time) is $t\approx 3$ sec. Such powers will be achieved in the near future using, for example, CO_2 or CO lasers. However, it should be noted that the fast acceleration of relatively light vehicles in the atmosphere by laser jet engines can be performed more readily with laser air-breathing engines.

The main advantage of laser air-breathing jet engines over all others is that the propellant is atmospheric air and, therefore, the final mass of the vehicle M_k is equal to its initial mass M_0. Moreover, because of the simplicity of the operation of such an air-breathing engine (we are speaking here of the pulse-periodic variant discussed above) one may approach a situation in which the payload of a flight vehicle is close to its total mass M_0. Consequently, relatively small thrusts $F_{av}\sim 1000$ kgf would be sufficient to achieve high initial accelerations of flight vehicles (for example, to several tens of g). According to our estimates, a thrust of ~1000 kgf would require the same average laser power $P_{av}\sim 10^7$ W,

as in the case of a laser jet engine with the evaporation mechanism. It should be noted that for $P_{av} = 10^7$ W and laser pulse repetition frequency $1/\tau_1 \approx 300$ Hz the energy in each laser pulse should be $E \approx 30$ kJ; then, according to our estimates, the maximum diameter of the calculated reflector is $D_{max} \approx 70$ cm.

The authors are grateful to B. V. Bunkin, A. I. Barchukov, and V. I. Konov for discussing various subjects considered in our paper.

[1]G. A. Askar'yan and E. M. Moroz, Zh. Eksp. Teor. Fiz. **43**, 2319 (1962) [Sov. Phys. JETP **16**, 1638 (1963)].
[2]S. I. Anisimov, Ya. A. Imas, G. S. Romanov, and Yu. V. Khodyko, Deĭstvie izlucheniya bol'shoĭ moshchnosti na metally (Effects of High-Power Radiation on Metals), Nauka, M., 1970.
[3]Yu. V. Afans'ev and O. N. Krokhin, Tr. Fiz. Inst. Akad. Nauk SSSR **52**, 118 (1970).
[4]V. A. Batanov, F. V. Bunkin, A. M. Prokhorov, and V. B. Fedorov, Zh. Eksp. Teor. Fiz. **63**, 586 (1972) [Sov. Phys. JETP **36**, 311 (1973)]; A. M. Prokhorov, V. A. Batanov, F. V. Bunkin, and V. B. Fedorov, IEEE J. Quantum Electron. **QE-9**, 503 (1973).
[5]J. F. Ready, Effects of High Power Laser Radiation, Academic Press, New York, 1971 (Russ. Transl. Mir., M., 1974).
[6]A. Kantrowitz, Astronaut. Aeronaut. **9**, No. 3, 34 (1971); 10, No. 5, 74 (1972).
[7]A. N. Pirri, M. J. Monsler, and P. E. Nebolsine, AIAA J. 12, 1254 (1974).
[8]A. I. Barchukov, F. V. Bunkin, V. I. Konov, and A. M. Prokhorov, Pis'ma Zh. Eksp. Teor. Fiz. **23**, 237 (1976) [JETP Lett. **23**, 213 (1976)].
[9]A. I. Barchukov, F. V. Bunkin, V. I. Konov, and A. M. Prokhorov, Pis'ma Zh. Eksp. Teor. Fiz. **17**, 413 (1973) [JETP Lett. **17**, 294 (1973)].
[10]A. N. Pirri, R. Schlier, and D. Northam, Appl. Phys. Lett. 21, 79 (1972).
[11]J. E. Lowder, D. E. Lencioni, T. W. Hilton, and R. J. Hull, J. Appl. Phys. **44**, 2759 (1973).
[12]A. I. Barchukov, F. V. Bunkin, V. I. Konov, and A. A. Lyubin, Zh. Eksp. Teor. Fiz. **66**, 965 (1974) [Sov. Phys. JETP **39**, 469 (1974)].
[13]A. I. Barchukov, F. V. Bunkin, N. V. Karlov, V. I. Konov, and G. P. Kuz'min, v kn. Tezisy dokladov VII Vsesoyuznoĭ konferentsii po kogerentnoĭ i nelineĭnoĭ optike, Tashkent, 1974 (Abstracts of Papers presented at Eighth All-Union Conf. on Coherent and Nonlinear Optics, Tashkent, 1974).
[14]J. E. Lowder and L. C. Pettingill, Appl. Phys. Lett. **24**, 204 (1974).
[15]J. F. Ready, Appl. Phys. Lett. **25**, 558 (1974).
[16]S. A. Metz, L. R. Hettche, R. L. Stegman, and J. T. Schriempf, J. Appl. Phys. **46**, 1634 (1975).
[17]L. D. Landau and E. M. Lifshitz, Statisticheskaya fizika, Nauka, M., 1964 (Statistical Physics, 2nd ed., Clarendon Press, Oxford, 1969).
[18]S. A. Ramsden and P. Savic, Nature (London) **203**, 1217 (1964).
[19]F. V. Bunkin, V. I. Konov, A. M. Prokhorov, and V. B. Fedorov, Pis'ma Zh. Eksp. Teor. Fiz. **9**, 609 (1969) [JETP Lett. **9**, 371 (1969)].
[20]Yu. P. Raĭzer, Lazernaya iskra i rasprostranenie razryadov, Nauka, M., 1974 (Laser-Induced Discharge Phenomena, Plenum Press, New York, in preparation).
[21]L. D. Landau and E. M. Lifshitz, Mekhanika sploshnykh sred, Gostekhizdat, M., 1954 (Fluid Mechanics, Pergamon Press, London, 1959).
[22]Ya. B. Zel'dovich and Yu. P. Raĭzer, Fizika udarnykh voln i vysokotemperaturnykh gidrodinamicheskikh yavleniĭ, Nauka, M., 1966 (Physics of Shock Waves and High-Temperature Hydrodynamic Phenomena, 2 vols, Academic Press, New York, 1966/67).
[23]V. A. Batanov, F. V. Bunkin, A. M. Prokhorov, and V. B. Fedorov, Pis'ma Zh. Eksp. Teor. Fiz. **11**, 113 (1970) [JETP Lett. 11, 69 (1970)]; Zh. Eksp. Teor. Fiz. **63**, 1240 (1972). [Sov. Phys. JETP **36**, 654 (1973)].
[24]V. A. Batanov, V. A. Bogatyrev, N. K. Sukhodrev, and V. B. Fedorov, Zh. Eksp. Teor. Fiz. **64**, 825 (1973) [Sov. Phys. JETP **37**, 419 (1973)].
[25]L. I. Sedov, Mekhanika sploshnoĭ sredy (Mechanics of Continuous Media), Vol. 2, Nauka, M., 1970.
[26]L. I. Sedov, Metody podobiya i razmernosti v mekhanike (Similarity and Dimensional Methods in Mechanics), Nauka, M., 1967.

Translated by A. Tybulewicz